

RSC Advances



This is an *Accepted Manuscript*, which has been through the Royal Society of Chemistry peer review process and has been accepted for publication.

Accepted Manuscripts are published online shortly after acceptance, before technical editing, formatting and proof reading. Using this free service, authors can make their results available to the community, in citable form, before we publish the edited article. This *Accepted Manuscript* will be replaced by the edited, formatted and paginated article as soon as this is available.

You can find more information about *Accepted Manuscripts* in the [Information for Authors](#).

Please note that technical editing may introduce minor changes to the text and/or graphics, which may alter content. The journal's standard [Terms & Conditions](#) and the [Ethical guidelines](#) still apply. In no event shall the Royal Society of Chemistry be held responsible for any errors or omissions in this *Accepted Manuscript* or any consequences arising from the use of any information it contains.

ARTICLE

Effect of the Presence of Titania Nanoparticles in the Development of *Pseudomonas fluorescens* biofilms on LDPE

Cite this: DOI: 10.1039/x0xx00000x

Received 00th January 2012,
Accepted 00th January 2012

DOI: 10.1039/x0xx00000x

www.rsc.org/J.M. Arroyo^a, D. Olmos^a, B. Orgaz^b, C.H. Puga^b, C. SanJose^b, J. González-Benito^a

In this study the use of TiO₂ nanoparticles in the preparation of active packaging film materials is investigated. High energy ball milling was used to uniformly disperse TiO₂ nanoparticles within low density polyethylene, LDPE. Differential scanning calorimetry (DSC) and scanning electron microscopy (SEM) were used to characterize the nanocomposites. Growth of *Pseudomonas fluorescens* and subsequent bio-film formation on the surfaces of LDPE with and without TiO₂ nanoparticles were studied with Atomic Force Microscopy (AFM) and viable cell count. A set of samples placed either facedown or face-up in microwell plates were subsequently immersed in *P. fluorescens* cultures and incubated up to 48h at 4 or 30°C. AFM images shown that the presence of titania nanoparticles affects the growth, size, distribution and arrangement of bacteria on the polymer surfaces. Cell recovery and counting experiments revealed a reduction of at least 1-Log (i.e. 90% reduction) in bacterial colony forming units per square centimeter (cfu/cm²) at the TiO₂ nanofilled polymer compared to LDPE films, without photoactivation. In the presence of TiO₂ nanoparticles, bacterial cells attached to the surfaces formed tight aggregates with apparently minor amount of “extracellular polymer substances” (EPS) around.

Introduction

The aim of food packaging is basically to constitute a physical barrier between food and the environment to protect, avoid or slow down food deterioration, extending its shelf-life and assuring consumer's safety. The increasing development of nanotechnology has dramatically changed the concept of food packaging from the merely “passive barriers” used in the past towards the so-called “active packaging”. Indeed the development of new smart packaging materials to optimize product shelf-life and quality has been the goal of many companies. These products are based on multifunctional materials that are able to interact with food to respond to harsh environmental conditions or even alert the customer if food is contaminated. In this sense, nanotechnology can help industry to achieve these challenges. For instance, it is possible to modify the behavior of polymer films used for wrapping with the addition of certain type of nanoparticles. This might increase barrier and other physico-chemical properties (mechanical, thermal and antimicrobial).

Probably, among the above mentioned, new plastic materials (polymers and composites) with bactericidal or bacteriostatic effect are the most promising systems for agriculture and food industry¹. Essentially, the antimicrobial agent is directly introduced into the packaging material to prevent or delay bacterial growth on the food's surface where the alteration or degradation process begins.² Research in this

area has mainly focused on the development of composite materials using nanoparticles of silver or zinc oxide.^{3,4} The antimicrobial activity of titanium dioxide (TiO₂, mainly photocatalyzed by UV light) is well known. This activity was discovered by Matsunaga *et al.*⁵ and since then it has been used to degrade organic pollutants and deactivate a broad spectrum of microorganisms.⁶ Recent investigations have studied the direct incorporation of TiO₂ in films of ethylene vinyl alcohol,⁷ isotactic polypropylene,⁸ low density polyethylene⁹ and polycaprolactone.¹⁰ Although the activity of TiO₂ is simultaneously combined with the irradiation of UV light, recent studies suggest that TiO₂ can also affect bacterial growth in the absence of UV light.¹¹⁻¹³ Therefore, one possible alternative to obtain polymer nanocomposites useful for preparing “active packaging” materials is to incorporate TiO₂ nanoparticles in polymer matrices.¹⁴⁻¹⁶

Atomic force microscopy (AFM) has been revealed as one of the most relevant techniques for materials characterization and has played an important role in the field of biological sciences and more specifically in microbiology. In particular, from the point of view of microbiology, it has evolved from a merely visualization technique to a quantitative molecular toolkit that allows scientists for instance examining the physicochemical properties of cell membranes.¹⁷ Besides, AFM has also shown a great potential for rapid qualitative detection of microorganisms what is crucial for food safety and quality.¹⁸ AFM offers better resolution than optical microscopy and it

may complements scanning electron microscopy (SEM) since sample preparation is minimal or nil (Yang and Wang, 2008).¹⁸

Free living microorganisms can colonize surfaces forming so-called biofilms, communities of sessile cells embedded in a sticky gel of hydrated extracellular macromolecules produced by themselves, that binds them to a substratum surface. In this form, cells are protected from adverse conditions, such as those involved in sanitation. Biofilms are easily formed on surfaces in contact with food (equipment, utensils, packaging etc) from which they can contaminate it and compromise its safety and quality.¹⁹ *Pseudomonas fluorescens* was here selected as a biofilm forming organism since it is one of the microorganisms most frequently associated with food spoilage under refrigeration temperatures. The aim of this work was to study the antimicrobial and/or antiadhesive activity of low density polyethylene (LDPE) films filled with TiO₂ nanoparticles (20% wt) in the absence of light. Biofilm formation was studied at two temperatures, 4°C and 30°C, using two experimental system configurations in order to study the influence of gravity on cell attachment. The antibiofilm behavior or the materials here prepared was both checked by viable cell counting and by AFM inspection of the exposed surfaces.

Experimental

Materials

Commercial LDPE (melt index 25.00 g/10 min, 190°C/2.16 kg, ASTM D 1238, and density = 0.93 g cm⁻³) and TiO₂ nanoparticles (average diameter 65 nm) used in this work were supplied by Aldrich.

High energy ball milling

The materials in powder form were blended using a commercial mixer Retsch MM400 under cryogenic conditions. The samples were introduced in two stainless steel vessels of 50 ml with one milling ball of 2.5 cm diameter each. The samples consisted on LDPE (control) and LDPE filled with 20% of TiO₂ nanoparticles (weight percentage) (LDPE-TiO₂). The filling level of the vessel is limited by the following settings: one third of the total volume is occupied by the sample, whilst other third is occupied by the ball. The remaining third is the free vessel volume, essential for the powder and ball motion during the agitation.

The milling process was done immersing the vessels filled with the sample and the milling ball in liquid nitrogen for 15 minutes. Next, the vessels were placed in the MM400 mixer milling machine and subjected to one milling cycle for 5 minutes using a vibration frequency of 28 kHz. This cycle was repeated 12 times to complete 1h of active milling. Previous results²⁰ point out that metal contamination arising from the milling tools due to the milling process was less than 0.5% by weight.

Films preparation

The films were prepared by placing the milled powders between two square sheets of polyimide (Kapton®) of 10×10cm². To control the thickness of the film, a mask of the same material was used with a window of 9 cm² where the powders were placed. The whole assembly, placed between twoTeflon sheets, was covered altogether with two aluminum plates (see Figure 1). To prepare the films, 120mg of material (LDPE or LDPE-TiO₂) were deposited inside the mold. This system was then heated in an oven at 150 °C for 1h, while under two weights of 5.6 kg to provide a constant pressure of

0.056 kg/cm². Then, the sample was left to cool down to room temperature still under the same constant pressure.

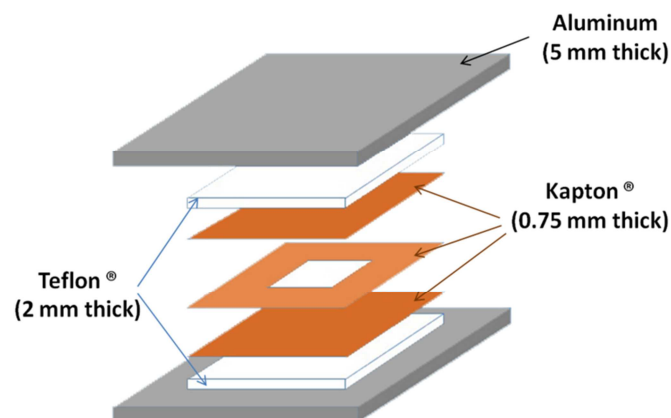


Fig. 1 Experimental setup used for film processing (LDPE, LDPE-TiO₂).

Differential scanning calorimetry

The non-isothermal crystallization and melting processes of both materials were studied in a Mettler Toledo 822E differential scanning calorimeter (DSC) under N₂ atmosphere. Previous thermal history of the samples was erased heating the samples at 20°C/min from 35 to 180 °C and holding this temperature for 5 min. After that, subsequent dynamics experiments were performed; (i) crystallization process cooling the samples from 180 to 35 °C at 20 °C/min and ii) melting process heating the samples from 35 °C to 180 °C at 20 °C/min. The experiments were carried out in DSC 50 µl aluminum pans weighting approximately 10 mg of the films previously prepared. To calculate the crystallization degree, X_c, the enthalpies of crystallization or fusion were used, ΔH (Eq. 1).

$$X = \frac{\Delta H / (1-x)}{\Delta H_m^0} \quad (1)$$

where x is the mass fraction of TiO₂ nanoparticles and ΔH_m⁰ is the enthalpy of fusion for the fully crystalline LDPE, ΔH_m⁰ = 289.9 J/g.²¹

Atomic force microscopy and scanning electron microscopy

Morphological characterization of the films and visualization of bacteria by atomic force microscopy was performed using a Multimode atomic force microscope Nanoscope IVA (Digital Instruments/ Veeco Metrology Group). All measurements were carried out at ambient conditions in tapping mode with etched silicon probes (stiffness 40 N/m). The driving frequency of the probe was adjusted to the resonant frequency in the immediate vicinity of the samples. The films roughness was determined on AFM images of 20 × 20 µm² dimensions. Image analysis was carried out with Nanoscope software 6.12r1.

To examine the distribution of TiO₂ nanoparticles in the composite film a SEM Philips XL30 equipped with an EDAX detector (energy dispersive X-ray analysis) DX4i was used. In all cases the samples were gold coated by sputtering procedure to make them conductive and avoid electrostatic charge accumulation.

Bacterial cultures, cell recovery and count

Pseudomonas fluorescens B52 used in this work was isolated from raw milk according to the method described by Richardson and

Te Whaiti²² and was stored in trypticase soy broth (TSB, Oxoid) with 10% glycerol at $-20\text{ }^{\circ}\text{C}$. Pre-inocula were cultured overnight in TSB at $30\text{ }^{\circ}\text{C}$. Cells were harvested by centrifugation at $4000 \times g$ for 10 min, washed twice in sterile TSB and their optical density at 600 nm (OD_{600}) adjusted by dilution with TSB to be used as inoculum, in order start the cultures with a cell density of $10^3\text{ CFU}\cdot\text{mL}^{-1}$.

Cultures for biofilm formation were performed in 24-well microplates (Thermo Fisher Scientific) using LDPE coupons as adhesion substrate. For their preparation, circular samples of the films were cut (6 mm diameter for AFM visualization and 10 mm diameter for cell recovery and counting) and fixed with an epoxy adhesive (92 NURAL, Henkel) onto AFM sample plates (12 mm diameter). In all cases, and prior to the incubations, samples were cleaned by spraying on a 70% solution of ethanol and subsequently drying in a sterile laminar flow hood. A total of seven independent experiments were conducted under different conditions as shown in Table 1.

Table 1. Conditions used for the bacterial cultures of the samples tested.

Experiment number	Temperature ($^{\circ}\text{C}$)	Time (h)	Coupon position	Coupon rinsing with 0.09% NaCl
1	4	24	Face down	NO
2-3	4	48	Face down	YES
4-7	30	24	Face up	YES

Two system configurations were used for biofilm development. The first one was used in experiments 1 to 3 (table 1). These film samples were horizontally fixed into the inner face of the microplate lid, held in this position with the help of magnetic tape and a magnet, so that the film was upside down. After closing the lid, the films were fully immersed in the culture medium (4.4 ml of TSB, which had been previously poured in the corresponding well). The second configuration was used in experiments 4 to 7. The samples were placed face up in the bottom of the wells, here face-up, which were filled up with TSB. Microplates, wrapped in aluminum foil to protect the samples from light, were placed into an incubator at the corresponding temperature under constant orbital shaking (50 rpm). After incubation time, the films were removed and in order to discard loosely attached cells, gently rinsed with sterile saline solution (NaCl 0.9% wt), except in experiment 1 where no washing was done. For microscopy visualization, rinsing was conducted by applying a few drops of saline solution on the film with a pipette, while for cell counting, coupons were briefly immersed in a saline solution and gently rocked. Samples to be visualized by AFM were stored in a humid environment at 4°C until observation within the next 48h.

For cell recovery and counting, the cells adhered to the surfaces of each material (LDPE or LDPE-TiO₂) were removed using a cotton swab and transferred into a 1.5 mL peptone water tube that was vigorously stirred in a vortex to break up cell aggregates, to be immediately diluted in peptone water and plated into trypticase soy agar (TSA, Oxoid) according to the drop method described by Hoben and Somasegaran²³. Colonies were counted after incubation at 30°C for 48h. Values shown are the average of 3 films of each sample processed for cell recovery and count.

Statistical analysis

The effects of the presence of TiO₂ nanoparticles in LDPE over bacterial growth were studied by one way variance analysis considering the run as a fixed effect according to the model:

$$y_{ij} = \mu + c_i + f_j + c_i \times f_j + \varepsilon_{ij} \quad (2)$$

where:

y_{ij} : bacterial concentration of sample j and run i

μ : general average

c_i : run i (from 4 to 7)

f_j : sample (LDPE, LDPE-TiO₂)

ε_{ij} : error of run i and sample j

In case the interaction $c_i \times f_j$ is not significant it was eliminated from the model and included within the error. This statistical analysis was carried out using the GLM procedure of SAS software. Effects of the factors were declared significant at $P < 0.05$.

Results and discussion

Influence of TiO₂ nanoparticles in crystallization and melting of LDPE observed by DSC

It is well known that final properties of semicrystalline polymers are dependent on its crystalline morphology and structure. Besides, surface free energy changes might alter final bacterial adhesion.^{24,25} One way to have some information about changes in crystallinity of LDPE under the influence of the presence of TiO₂ nanoparticles is to study its melting and crystallization process with and without particles. The melting and non-isothermal crystallization of the materials under study are shown in Figure 2. Clear differences between the DSC traces of the samples cannot be seen. In the crystallization process (Figure 2 bottom) there are two exothermic peaks, the main one at around 92°C and a secondary one at lower temperatures (50°C in LDPE and 43°C in LDPE-TiO₂). Crystallization occurs at 92°C what agrees with previous studies.²⁶ The presence of the secondary peak at lower temperatures has been attributed to a thermal relaxation process²⁷ although its microscopic origin is still unclear. In the melting process (Figure 2 top) there is one endothermic peak.

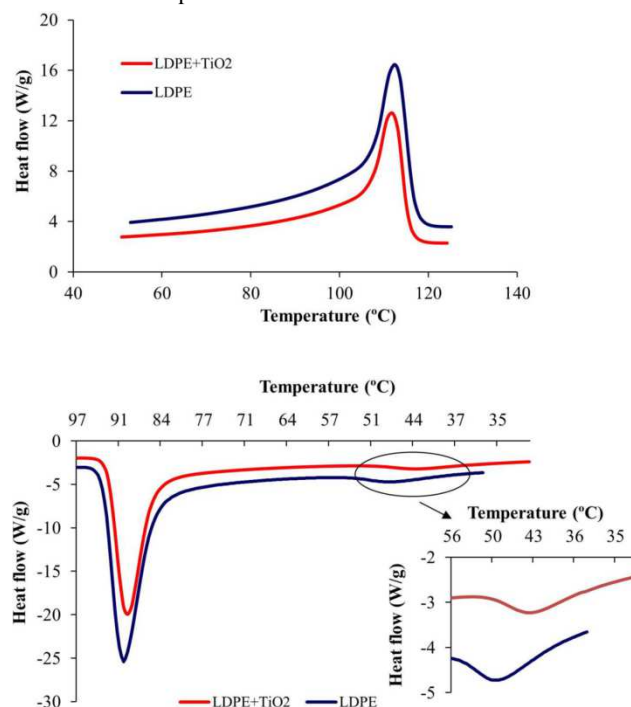


Fig. 2 DSC traces corresponding to the second heating scan (top) and to the cooling scan (bottom) of the films LDPE and LDPE-TiO₂.

In Table 2 all the parameters coming from the DSC analyses are collected. The presence of nanoparticles seems to affect the crystallization process. In fact, differences of about 4°C are shown in the crystallization temperature peak (Figure 2 bottom) and the same applies to the peak appearing at lower temperatures assigned to the thermal relaxation. This slight decrease in the crystallization temperature of LDPE-TiO₂ with respect to LDPE sample may be due to a restriction in the motion of macromolecular chains as a consequence of the presence of nanoparticles what might impede early ordering. On the other hand, no significant differences in the melting temperature peaks between the two materials (LDPE or LDPE-TiO₂) were observed, this being in good agreement with previous results on HDPE.²⁶ In the semicrystalline polymers context, this result is usually indicative of none structural or lamellar size changes. Furthermore, no significant differences were detected in the degree of crystallinity, suggesting that the presence of TiO₂ nanoparticles has not any influence on the amount of crystals present in the samples. Ma *et al.*²⁸ observed differences in the degree of crystallinity of LDPE blended with TiO₂ nanoparticles, but in that study the surface of the particles was modified by different treatments.

Table 2. DSC Parameters obtained for the first and second heating scans (melting) and for the cooling scan (crystallization) of the samples LDPE and LDPE-TiO₂.

Sample	1 st heating scan			2 nd Heating scan			Cooling scan		
	T _{mp} (°C)	ΔH _m (J/g)	X _c	T _{mp} (°C)	ΔH _m (J/g)	X _c	T _{sp} (°C)	ΔH _m (J/g)	X _c
LDPE	116.1	122.0	0.42	112.4	116.3	0.40	94.2	93.2	0.32
LDPE+TiO ₂	114.9	124.4	0.43	111.9	116.6	0.40	90.0	90.6	0.31

Therefore, DSC results suggest that possible effects on PF-B52 growth due to the presence of TiO₂ nanoparticles should not be a consequence of induced changes in LDPE crystallinity, structure and/or morphology.

Morphological analysis: SEM and AFM visualization of polymer surfaces

SEM micrographs in Figure 3 correspond to the surfaces of the films under study before exposure to the bacterial cultures. Figures 3 (a) and (c) show the micrographs obtained using the SE signal for both LDPE and LDPE-TiO₂. The surface of LDPE-TiO₂ seems rougher than that of pure LDPE, probably due to the presence of the particles near that region. On the other hand, BSE micrographs (Fig. 3 (b); Fig. 3(d)) showed a quite uniform dispersion of titania particles (represented by the brighter domains indicative of the presence of heavier elements such as Ti). However, there are some areas of variable size and shapes where aggregates seem to be present; this may be due to the high content of titania nanoparticles in the sample (20 % wt/wt).

Before exposure to the bacterial cultures, the topography of the films was also examined by AFM. In Figure 4, typical AFM images of LDPE and LDPE-TiO₂ samples are shown for which the most heterogeneous seems to be the later one. However, to have a clearer idea about the influence of the presence of TiO₂ particles on the topography of the films, roughness was determined calculating the roughness average (Ra) from 20×20μm² images, obtaining values of 21.2 and 27.2 nm for LDPE and LDPE-TiO₂, respectively. It is reasonable to think that a rougher surface should imply more available space for *P. fluorescens* B52 attachment, therefore, after the culture and in the absence of other effects, one would expect more bacteria on the nanofilled polymer.

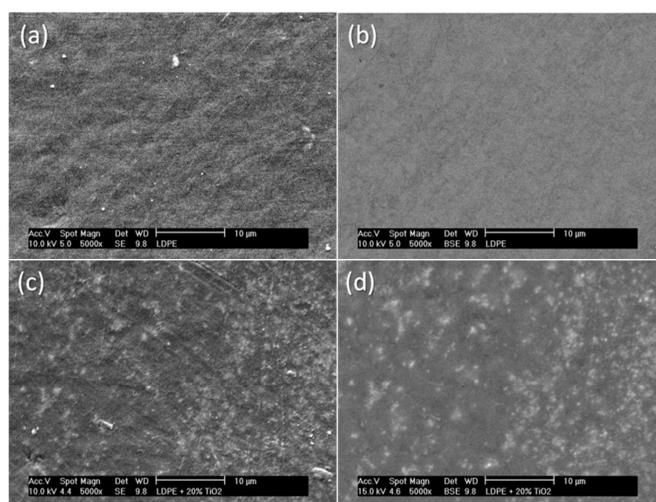


Fig. 3 SEM micrographs of the film surfaces for LDPE: (a) using SE signal and (b) using BSE signal or LDPE-TiO₂: (c) using SE signal and (d) using BSE signal.

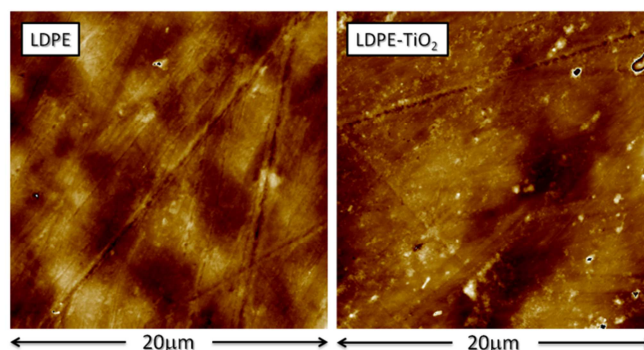


Fig. 4 Topography AFM images of the surface of LDPE and LDPE-TiO₂ samples before exposure to the bacterial cultures.

Biofilm formation on polymer surfaces

Bacterial cultures at 4°C

Figure 5 shows topographical images obtained by AFM of the films exposed to bacterial cultures corresponding to experiments 1 (top) and 2 (bottom) performed at low temperature (4°C). In all cases (experiments 1-3) a deposit formed by a kind of irregular shape particles of less than 3 micrometers is observed, not easily identifiable with the typical rod-like shape of *Pseudomonas* cells (about 1 μm in length). Considering the films of LDPE without particles longer culture times is translated into larger amount of deposited material as shown in Figure 5 (bottom). The fact that this sample was washed reinforced the above mentioned. On the other hand, when the LDPE were filled with TiO₂ nanoparticles the amount of deposit observed was smaller. In fact, for longer culture time and after washing almost no deposit was observed (Figure 5, LDPE-TiO₂ bottom).

The appearance of the deposit observed may be interpreted as an accumulation of bacteria embedded on the extracellular polymeric substances (EPS) produced by themselves. However, the neat geometric shapes do not fit well with the characteristic rod-like shape of *P. fluorescens* suggesting that a layer of the medium used for the culture (compare left vs. right images in Figure 5) is adhered to the surface of the films. Probably both, the system configuration

i.e., the samples were placed facedown to avoid the effect of gravity, and the low temperature/short incubation time have hampered biofilm development. The layer of material observed might correspond to the early stages of biofilm formation. Therefore, only the image in the bottom left of the Figure 5 could be certainly ascribed to a conventional biofilm image. The differences between the remaining images in Figure 5 and those in Figure 4 could be interpreted as “preconditioning” of the surfaces in Figure 5 with organic material from the culture medium, very rich in protein, possibly (but not certainly) topped by some weakly bound cells, which have been detached by the saline rinse applied to the Figure 5 bottom right sample.

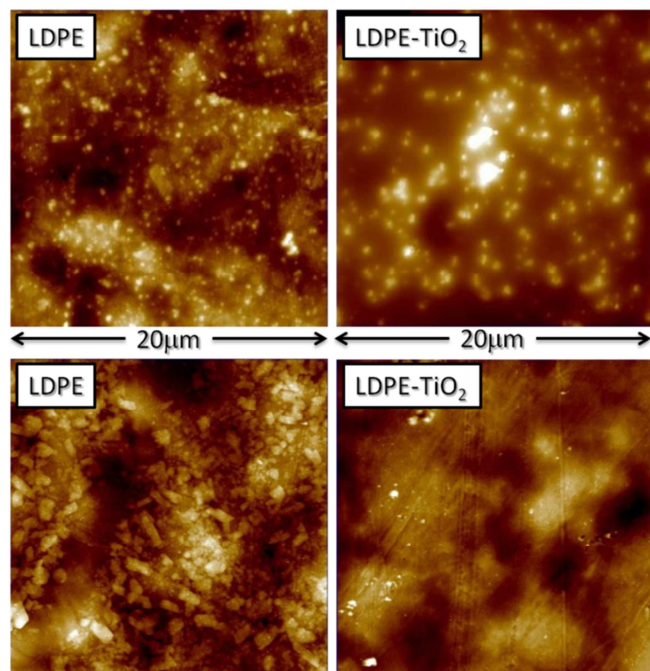


Fig. 5 AFM Topography images of the surface of films after bacterial cultures at 4 °C for 24h (Experiment 1, Top), and 48h (Experiment 2, Bottom). LDPE samples (images on the left) and LDPE-TiO₂ samples (images on the right).

Bacterial cultures at 30 °C

In Figure 6, AFM images of the samples after incubation experiments carried out at 30 °C are shown. The micrographs show advanced growth of bacteria on the surfaces of both films (LDPE and LDPE-TiO₂). In general, LDPE films filled with TiO₂ nanoparticles showed fewer amounts of bacteria attached to their surface though arranged in more densely packed aggregates. Besides, bacteria were arranged according to different patterns depending on the material. In LDPE films bacteria were homogeneously distributed throughout the whole surface, forming small and thin microcolonies, whereas on the LDPE-TiO₂ samples, bacteria appeared in tight, massive much larger colonies, being the rest of the surface almost uncovered. Microorganisms' aggregation in the presence of TiO₂ has also been described in other studies for bacteria of the genus *Streptococcus*²⁹ and *Escherichia coli*.³⁰ Although not yet demonstrated, one possible explanation for this may be that TiO₂ particles, which are positively charged, form bridges linking the negatively charged surface of bacterial cells, thus promoting tight cell aggregates.³¹ Another plausible is that TiO₂ nanoparticles due to the important bactericidal effect against *P. fluorescens* limits its growth to those regions where the

concentration of the particles is very low or null. Conversely, in the absence of TiO₂ nanoparticles bacteria have fewer arrangement restrictions for colonizing the whole surface.

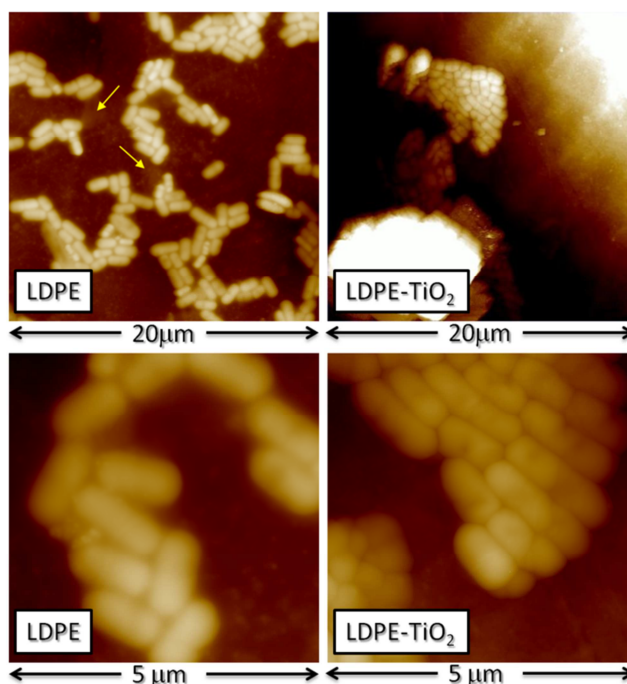


Fig. 6 AFM height images obtained on the surfaces of LDPE and LDPE-TiO₂ films covered with *P. fluorescens* cells developed at 30 °C.

Furthermore, bacteria growing on LDPE films were surrounded by extracellular material (probably EPS). However, this material did not appear when bacteria grew on the LDPE-TiO₂ films. This inhibition of EPS production by cells suggests, as pointed out elsewhere,¹⁶ that reduction and dense arrangement of bacteria on the surface of TiO₂ filled LDPE may be a consequence of the polysaccharides (EPS) degradation induced by the presence of titania. Additionally, Figure 7 shows a cross section profile of some specific regions of the samples presented in Figure 6 illustrate the actual size and dimensions of the bacteria. It can be observed that the bacteria grown in the presence of titania nanoparticles are slightly smaller than those grown in LDPE suggesting a clear effect of the nanoparticles on *P. fluorescens* metabolism. It may be significant that some of the bacteria attached to LDPE-TiO₂ films (Figure 6 bottom right) show some external deformations that could be an indicative of membrane damage. It is well known that positively charged biopolymers such as chitosan may interact with cell membrane causing cell damage and/or death. Indeed this biopolymer has shown good properties as antibiofilm agent.³²

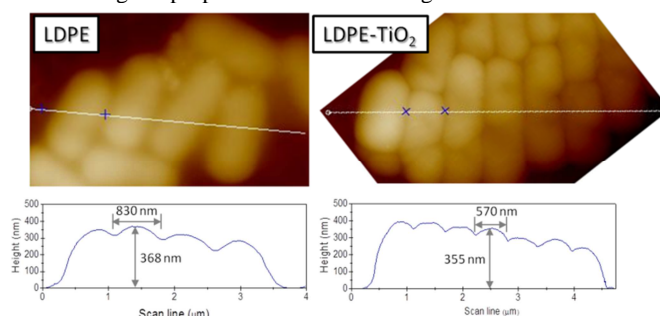


Fig. 7 Cross section profile of the 5µm images shown in Figure 6 for LDPE and LDPE-TiO₂.

Bacterial viable counts

The results of the four experiments (4-7) carried out to quantify bacterial growth on the surface of the films are shown in Figure 8. Bacterial attachment was significantly less on LDPE-TiO₂ than on LDPE films, at least 1-Log₁₀ lower. Results from trial 5, which appear more extreme than the rest, could be possibly due to an artifact, such as insufficient mechanical cell disaggregation before plating or particularly high concentration of TiO₂ particles in the coupons involved.

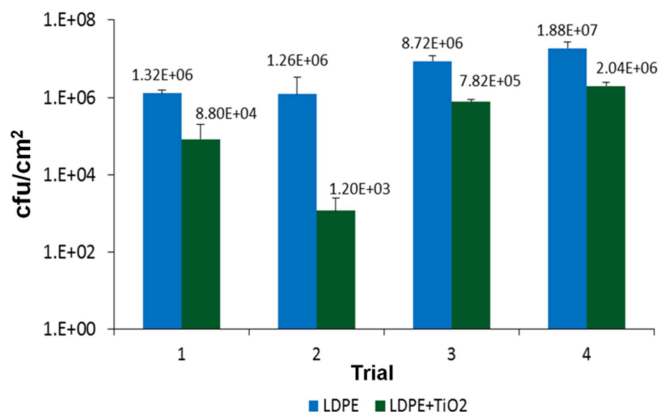


Fig. 8 *Pseudomonas fluorescens* growth on the surface of bare LDPE and LDPE containing TiO₂ films at 30°C/24h.

Many of the studies that have evaluated the bactericidal activity of TiO₂ did not find almost any effect in the absence of UV irradiation.^{33,34} However, there is also experimental evidence about TiO₂ affecting bacterial growth even under dark conditions. These studies were mainly performed on bacterial cultures where TiO₂ was added in solution form, but there are some works wherein TiO₂ has been incorporated into plant polymers as in the work of¹⁴ who prepared cellulose foils coated with TiO₂ nanoparticles and obtained a reduction in *Escherichia coli* viability up to 79 % for. As for synthetic polymers, Jiang and Zeng¹⁵ prepared polystyrene microspheres coated with TiO₂ achieving *Escherichia coli* mortality above 55 % after 2h exposure. Nieto *et al.*¹⁶ showed a significant reduction in the area covered by *Pseudomonas* biofilms on composites based on polystyrene filled with TiO₂ nanoparticles as well as an apparent decrease in the amount of extracellular polymeric substances secreted by this microorganism.

Previous works have suggested that the mechanism of action of TiO₂ is based on its ability for dehydrogenation and dehydration of organic compounds at high temperatures.³³ Furthermore, Gurr *et al.*³⁴ observed that the contact of bronchial epithelial cells with TiO₂ nanoparticles under dark conditions induced oxidative DNA damage, lipid peroxidation, micronucleus formation and increases in the production of hydrogen peroxide and nitric oxide in the absence of photocatalytic reaction. Zhukova *et al.*³¹ observed that under certain conditions *E. coli* tended to form aggregates in the presence of TiO₂ nanoparticles. These aggregates resemble the ones obtained or observed in our experiments. These authors observed besides that the antimicrobial effect of TiO₂ was higher when using high initial cell density (10⁸ CFU/mL) cultures of *E. coli*, that is, cultures in stationary phase, where physiological cell death and EPS degradation could be combined with TiO₂ effects. In comparison, the conditions used in the experiments presented here correspond to cultures still in exponential phase of growth, what might be the cause for more moderate TiO₂ effects. Differences in experimental conditions, including amount of TiO₂, may be behind the lack of response in the absence of UV light illumination. The results of this

study therefore are promising to show bactericidal potential of TiO₂ in absence of UV light and can be used for developing new antimicrobial packaging materials.

Conclusions

The results of this study evidenced bactericidal potential of TiO₂ nanoparticles in absence of UV light when they are within LDPE. Results suggest 90% decrease in the growth and development of *P. fluorescens* biofilms on the surfaces of polymer samples with titania nanoparticles is due to extracellular polymeric substances reduction and/or cell damage. The use of atomic force microscopy proved to be useful to reveal early stage development of biofilms as well as for helping to understand some possible outcomes of exposure to antimicrobial compounds. This study is a starting point for the development of new smart packaging materials with antimicrobial properties.

Acknowledgements

Authors gratefully acknowledge financial support of the Spanish Ministries of Science and Innovation (MAT2010-16815) and Economy and Competition (AGL2010-22212-C02-0).

Notes and references

^a Department of Materials Science and Engineering and IQMAAB. Universidad Carlos III de Madrid. Av. Universidad 30, 28911 Leganés (Spain). E-mail: javid@ing.uc3m.es.

^b Department of Nutrition, Food Science and Technology, Faculty of Veterinary, University Complutense of Madrid, 28040 Madrid, Spain.

References

- H.M.C. Azeredo H.M.C., *Trends Food Sci. Technol.*, 2013, **29**, 56-69.
- P. Appendini and J.H. Hotchkiss, *Innov. Food Sci. Emerg. Technol.*, 2002, **3**, 113-126.
- B.P. Chang, H.M. Akil, R.M. Nasir and S. Nurdijati, *J. Thermoplast. Compos. Mater.*, 24, 653-667.
- A.S. Dehnavi, A. Aroujalian, A. Raisi and S. Fazel, *J. Appl. Polym. Sci.*, 2013, **127**, 1180-1190.
- T. Matsunaga, R. Tomodam, T. Nakajima and H. Wake, *FEMS Microbiol. Lett.*, 1985, **29**, 211-214.
- C. Chawengkijwanich and Y. Hayata, *Inter. J. Food Microbiol.*, 2008, **123**, 288-292.
- M.L. Cerrada, C. Serrano, M. Sánchez-Chaves, M. Fernández-García, F. Fernández-Martín, A. de Andrés, R.J. Jiménez Riobóo, A. Kubacka, M. Ferrer and M. Fernández-García, *Adv. Funct. Mater.*, 2008, **18**, 1949-1960.
- A. Kubacka, M. Ferrer, M.L. Cerrada, C. Serrano, M. Sánchez-Chaves, M. Fernández-García, A. de Andrés, R.J. Jiménez Riobóo, F. Fernández-Martín and M. Fernández-García, *Appl. Catal. B-Environ.*, 2009, **89**, 441-447.
- H. Bodaghi, Y. Mostofi, A. Oromiehie, Z. Zamani, B. Ghanbarzadeh, C. Costa, A. Conte and M.A. Del Nobile, *LWT-Food Sci. Technol.*, 2013, **50**, 702-706.
- A. Muñoz-Bonilla, M.L. Cerrada, M. Fernández-García, A. Kubacka, M. Ferrer and M. Fernández-García, *Inter. J. Mol. Sci.*, 2013, **14**, 9249-9266.
- L.K. Adams, D.Y. Lyon, J.J. Pedro and P.J.J. Alvarez, *Water Res.*, 2006, **40**, 3527-3532.

- 12 A.I. Gomes, J.C. Santos, V.J.P. Vilar and R.A.R. Boaventura, *Appl. Catal. B-Environ.*, 2009, **88**, 283-291.
- 13 R. Van Grieken, J. Marugán, C. Pablos, L. Furones and A. López, *Appl. Catal B-Environ.*, 2010, **100**, 212-220.
- 14 W.A. Daoud, J.H. Xin and Y.H. Zhang, *Surf. Sci.*, 2005, **599**, 69-75.
- 15 G. Jiang and J. Zeng, *J. Appl. Polym. Sci.*, 2010, **116**, 779-784.
- 16 I. Nieto, D. Olmos, B. Orgaz, D.K. Bozanic, J. González-Benito, *Mater. Lett.*, 2014, **127**, 1-3.
- 17 V. Dupres, D. Alsteens, G. Andre and Y.F. Dufrêne, *Trends Microbiol.*, 2010, **18**, 397-405.
- 18 H. Yang and Y. Wang, *J. Food Sci.*, 2008, **73**, N44-N50.
- 19 D. Olmos, E. Rodríguez-Gutiérrez, J. González-Benito, *Polym. Comp.*, 2012, **33**, 2009-2021.
- 20 S. Srey, I.K. Jahid and S.D. Ha, *Food Control*, 2013, **31**, 572-585.
- 21 L. Mandelkern, Crystallization of polymers. In: Equilibrium concepts. 2002, 2nd edition, vol 1. New York: Cambridge University Press pp 259.
- 22 B.C. Richardson and I.E. Te Whaiti, *New Zealand J. Dairy Sci. Technol.*, 1978, **13**, 172-176.
- 23 H.J. Hoben, P. Somasegaran, 1982. *Appl. Environ. Microbiol.*, 1982, **44**, 1246-1247.
- 24 H.H. Tuson and D.B. Weibel, *Soft Matter*, 2013, **9**, 4368-4380.
- 25 P. Decuzzi and M. Ferrari, *Biomaterials*, 2010, **31**, 173-179.
- 26 D. Olmos, C. Domínguez, P.D. Castrillo and J. González-Benito, *Polymer*, 2009, **50**, 1732-1742.
- 27 Y. Men, J. Riege, H.R. Endeler and D. Lilge, *Macromolecules*, 2003, **36**, 4689-4691.
- 28 D. Ma, D., A. Yvonne, Y. Li, R.W. Siegel and L.S. Schadler, *J. Polym. Sci. Part B: Polym. Phys.*, 2005, **43**, 488-497.
- 29 T. Saito, T. Iwase, J. Horie and T. Morioka, *J. Photochem. Photobiol. B: Biology*, 1992, **14**, 369-379.
- 30 A. Simon-Deckers, S. Loo, M. Mayne-L'Hermite, N. Herlin-Boime, N. Menguy, C. Reynaud, B. Gouget and M. Carriere, *Environmen. Sci. Technol.*, 2009, **43**, 8423-8429.
- 31 LV. Zhukova, J. Kiwi and V.V. Nikandrov, *Colloids Surf. B: Biointerfaces*, 2012, **97**, 240-247.
- 32 B. Orgaz, M.M. Lobete, C.H. Puga and C. San Jose, *Inter. J. Molec. Sci.*, 2011, **12**, 817-828.
- 33 T. Reztsova, C.H. Chang, J. Koresh and H. Idriss, *J. Catal.*, 1999, **185**, 223-235.
- 34 J.R. Gurr, A.S. Wang, C.H. Chen and K.Y. Jan, *Toxicology*, 2005, **213**, 66-73.